Machine learning ATR-FTIR spectroscopy data for the screening of collagen for ZooMS analysis and mtDNA in archaeological bone

Manasij Pal Chowdhury, Kaustabh Datta Choudhury, Geneviève Pothier Bouchard, Julien Riel-Salvatore, Fabio Negrino, Stefano Benazzi, Ludovic Slimak, Brenna Frasier, Vicki Szabo, Ramona Harrison, et al.

Contents lists available at ScienceDirect

Journal of Archaeological Science

journal homepage: http://ees.elsevier.com

Machine learning ATR-FTIR spectroscopy data for the screening of collagen for ZooMS analysis and mtDNA in archaeological bone

Manasij Pal Chowdhury [a,b], Kaustabh Datta Choudhury [c], Geneviève Pothier Bouchard [d], Julien Riel-Salvatore [d], Fabio Negrino [e], Stefano Benazzi [f], Ludovic Slimak [g], Brenna Frasier [h], Vicki Szabo [i], Ramona Harrison [j], George Hambrecht [k], Andrew C. Kitchener [l], Roy A. Wogelius [b], Michael Buckley [a,b,*]

[a] Manchester Institute of Biotechnology, School of Natural Sciences, University of Manchester, 131 Princess Street, Manchester, M1 7DN, UK
[b] Interdisciplinary Centre for Ancient Life, School of Natural Sciences, University of Manchester, M13 9L, UK
[c] Independent Data Scientist, Bangalore 560095, India
[d] Département d'anthropologie et Laboratoire d'archéologie de l'Anthropocène, Université de Montréal, Canada
[e] Dipartimento di Antichità, Filosofia, Storia, Università degli Studi di Genova, Italy
[f] Università di Bologna, Dipartimento di Beni Culturali, Via degli Ariani 1, 48121, Ravenna, Italy
[g] CNRS, UMR 5608, TRACES, Université Toulouse -Jean Jaurès, Maison de la Recherche Bât 26, 5 allée Antonio Machado, 31058, Toulouse, France
[h] Biology Department, Saint Mary's University, 923 Robie Street, Halifax, Nova Scotia, B3Z 1B4, Canada
[i] History Department, 225 McKee, Western Carolina University, Cullowhee, NC 28723, USA
[j] University of Bergen, Bergen, Norway
[k] Department of Anthropology, University of Maryland, 1111 Woods Hall, 4302 Chapel Lane, College Park, MD 20742, UK
[l] Department of Natural Sciences, National Museums Scotland, Chambers Street, Edinburgh, EH1 1JF, UK

ARTICLE INFO

Keywords
Ancient biomolecules
Screening
Machine learning
Random forest
ATR-FTIR
DNA
ZooMS

ABSTRACT

Faunal remains from archaeological sites allow for the identification of animal species the enables the better understanding of the relationships between humans and animals, not only from their morphological information, but also from the ancient biomolecules (lipids, proteins, and DNA) preserved in these remains for thousands and even millions of years. However, due to the costs and efforts required for ancient biomolecular analysis, there has been considerable research into development of accurate and efficient screening approaches for archaeological biomolecular analysis. FTIR spectroscopy is one such approach that has been considered for screening of proteins, but its widespread use has been hindered by the fact that its predictive accuracy can vary widely depending on the extent of sample preservation and the instrument used. Further, screening methods for ancient DNA (aDNA) analysis are scarce. Here we present a new approach to vastly improve upon FTIR-based screening methods prior to ZooMS and aDNA analysis through the use of random forest-based machine learning. To do so, we use ATR-FTIR to examine three sets of archaeological bone assemblages and analyse them by ZooMS (Zooarchaeology by Mass Spectrometry; for taxonomic identification). Two of these are from Palaeolithic contexts, dominated by terrestrial fauna and include specimens with a variety of preservational conditions. The third set consists of Holocene faunal remains, with variable levels of preservation and is dominated by cetaceans. Using the Holocene faunal remains, we were able to more consistently evaluate ATR-FTIR based screening for mtDNA as well as ZooMS success. We report the first successful use of machine learning in ATR-FTIR-based screening technique for ancient mtDNA analysis, and our machine learning models conclusively improve the accuracy prior to usage of ATR-FTIR-based screening for ZooMS by 20–40%. The results also suggest this approach potentially allows for a universal screening system, applicable across multiple sites and largely independent of the spectrometers used.

* Corresponding author. Manchester Institute of Biotechnology, School of Natural Sciences, University of Manchester, 131 Princess Street, Manchester, M1 7DN, UK.
E-mail address: mbuckley82@gmail.com (M. Buckley)

https://doi.org/10.1016/j.jas.2020.105311
Received 1 July 2020; Received in revised form 7 November 2020; Accepted 14 December 2020
Available online xxx
0305-4403/

1. Introduction

Bone is a heterogenous biocomposite material, consisting of a mineral phase and an organic phase. Almost one hundred years ago, the mineral component of bone was shown to be similar to geologic hydroxyapatite ($Ca_5(PO_4)_3(OH)$) using X-ray diffraction (de Jong, 1926). However, later studies showed that the Ca/P molar ratios in bones is distinct from that of geological hydroxyapatite, and it has been considered that the mineral phase should be more accurately described as a highly disordered and substituted version of hydroxyapatite, with a high degree of carbonate substitution and OH deficiency in the crystal lattice (Boskey, 2007); the hydroxyapatite crystals are associated with an organic matrix which forms a scaffold for the crystal deposition. The organic matrix is dominated by collagen, a fibrous protein (~90% tyie I collagen), with non-collagenous proteins constituting approximately 5% and an even smaller amount of lipids (~2%) (Boskey, 2013). This composite matrix, with a large number of cells (the four types of cells being osteoblasts, bone lining cells, osteocytes, and osteoclasts) and blood vessels embedded in it collectively forms bone.

Bones are among the most widely discovered resource in archaeological sites and they provide a plethora of information of archaeological and paleontological interest. Faunal analysis in archaeology (zooarchaeology) allows us to understand the relationship between humans and animals, such as the economic exploitation of both wild and domesticated animals (Halstead and Isaakidou, 2017; Tornero et al., 2017), mapping the timeline of animal domestication (Napierala and Uerpmann, 2012; Perkins, 1973; Zeder and Hesse, 2000), understanding animal husbandry and livestock rearing practices (Bläuer and Kantanen, 2013; Samei et al., 2019; Stiner et al., 2014), and identifying hunting strategies by ancient humans (Marín et al., 2017; Yeomans et al., 2019). Over the past few decades, stable isotope analysis has become an important part of zooarchaeological analysis, providing information about dietary pattern (Kusaka, 2019; Lewis and Sealy, 2018; Schoeninger, 2014; van der Merwe and Vogel, 1978), palaeoclimate and palaeoecological reconstruction (Rofes et al., 2015; Stephan, 2000), and herd management in antiquity (Bocherens et al., 2001). Zooarchaeological analysis can also provide detailed information about societal structures in antiquity, including socioeconomic differences, and trade and exchange relations (Crabtree, 1990; Reitz, 1987; Somerville et al., 2010; Zeder, 1991). Studies analysing bone modification and culinary processing allows us to obtain valuable information about the evolution of humans by comparing food processing between various early hominins (Domínguez-Rodrigo et al., 2014; Ungar, 2004). Further, analysis of bones can also provide information extending beyond the archaeological and into the palaeontological period, providing us with knowledge about evolution and extinction of animals, including hominin evolution (Gruss and Schmitt, 2015; Herries et al., 2020; Ward and Hill, 1987).

Bone diagenesis refers to a complex set of physico-chemical changes that happens to archaeological bones during burial, and was originally defined on the basis of four diagenetic parameters: histological index, protein content, crystallinity, and bone porosity (Hedges et al., 1995). It was postulated that two main mechanism operate in bone diagenesis: the initial process is initiated by collagen hydrolysis, which is then followed by attack by micro-organisms which further increases the pore size and the surface area, further increasing the rate of chemical reactions, and ultimately the rate of diagenesis (Nielsen-Marsh and Hedges, 1999; Turner-Walker and Parry, 1995). The loss of collagen is also accompanied by an increase in the crystallinity (Weiner and Bar-Yosef, 1990; Wright and Schwarcz, 1996), which is further affected by chemical changes (ionic exchanges of fluorite or carbonate etc.) and the potential dissolution and re-precipitation of hydroxyapatite (Collins et al., 2002; Nielsen-Marsh and Hedges, 2000). During diagenesis, the ratio of carbonate-to-phosphate in the bone also changes, as carbonate can be incorporated in the bone during dissolution and re-crystallization, replacing either biogenic carbonate or phosphate ions (Lee-Thorp et al., 1989; LeGeros, 1981). A competing process includes loss of carbonate during dissolution, with both processes affecting the carbonate content and ultimately the crystal structure and stability of the mineral phase (LeGeros, 1981; Newesely, 1989).

The degradation of collagen in bones can take place through two modes: microbial degradation, and chemical degradation (primarily by hydrolytic pathways; Collins et al., 2002, 1995; Newesely, 1989; Nielsen-Marsh and Hedges, 2000). This chemical degradation is thought to proceed by hydrolytic cleavage of peptide bonds, followed by a dissolution of the short peptide fragments (Collins et al., 1995). The microbial attack is considered to be one of the early phases of bone diagenesis, and is often one of the major contributors to bone diagenesis and degradation of organic matter (Collins et al., 2002; Nielsen-Marsh and Hedges, 2000).

DNA too has limited chemical stability, and after cell death, is degraded by the action of nuclease and degraded by microorganisms (Lindahl, 1993). For ancient DNA, it has been postulated that the initial degradation results in the formation of shorter fragments by hydrolysis, which further decays by depurination and other forms of oxidative damage (involving both chemical and microbial pathways; Eglinton and Logan, 1991; Lindahl, 1993). The depurination is thought to be impeded by adsorption of DNA in hydroxyapatite, thereby reducing the rate of DNA degradation in bones (Lindahl, 1993; Okazaki et al., 2001). The binding of DNA to the collagen matrix has also been suggested (including formation of a collagen-DNA complex, or cross-linked with collagen, see (Kitamura et al., 1997)). This has been further supported by results which have showed that at least in some cases, the presence of DNA in archaeological bones can be linked to the crystallinity of the hydroxyapatite and the amount of collagen present (Götherström et al., 2002), with proteomic investigations more suggestive of mineral-bound influences (Wadsworth et al., 2017). Although the exact relationship between the collagen, hydroxyapatite and DNA is considered complicated and non-trivial, it has been suggested that DNA can survive in archaeological bones through four distinct processes: by binding with the collagen fibrils, by binding to the hydroxyapatite crystals as the bone mineralises, by getting adsorbed in the collagen fibrils as the unmineralized osteoid degrades, and by binding to the hydroxyapatite crystals during bone dissolution and re-crystallization (Campos et al., 2012).

Both microbial and physico-chemical degradation pathways are influenced by environmental conditions, with waterlogged conditions inhibiting microbial attack (see e.g. Bocherens et al., 1997). It has been argued that microbial attack is the most common mode of collagen loss in cool temperate climates, and hydrolytic mechanisms play an important part in hotter climates and for older bones (Collins et al., 2002). The temperature has remarkable influence on bone degradation, with colder temperatures both reducing the rate of reactions as well inhibiting microbial attacks. Other environmental factors such as the hydrology of the site and the geochemistry (presence of various soluble minerals, pH of the soil, etc.) also affect bone diagenesis, influencing the preservation both collagen and DNA (Collins et al., 2002; Gordon and Buikstra, 1981; Nielsen-Marsh et al., 2000, 2007). The ability to identify archaeological bones and to determine their species of origin is usually the first step in any zooarchaeological research, and has traditionally been done via morphological analyses, occasionally supplemented by techniques such as tooth wear analysis and isotope-based studies (e.g. Zeder et al., 2006). However, morphological analyses suffer from particular limitations, the most notable being the inability to identify highly fragmentary remains, which often lack identifiable morphological markers. Further, skeletal differences between certain taxa can be difficult to distinguish (for example between

sheep (*Ovis*) and goats (*Capra*), see Clutton-Brock, 1979; Payne, 1985). This problem is further compounded by the fact that taphonomic processes may erode certain diagnostic features (Munson, 2000).

Collagen peptide sequencing has been developed as a replicable and objective method to identify archaeological bones up to the genus (and sometimes the species) level. This approach, which is termed Zooarchaeology by Mass Spectrometry (ZooMS), involves the extraction of collagen from archaeological bones, enzymatic digestion to furnish tryptic peptides, and subsequent mass spectrometric identification of the peptides (Buckley et al., 2009, 2010). The ZooMS analysis can be performed on the either the soluble fraction of the collagen or the insoluble fraction (Buckley 2018), with the soluble fraction having the advantage that it potentially allows for the use of the insoluble fraction for isotopic analysis (e.g. radiocarbon analysis or stable isotopic analysis to determine dietary practices; Wadsworth and Buckley, 2018); ZooMS collagen fingerprinting itself also being suggested as a screening method for radiocarbon dating success (Harvey et al., 2016). Archaeological bones can also be identified by analysis of ancient DNA (aDNA). However, while this process can result in a more unambiguous identification of the species of origin, the process typically has a higher failure rate, and is more expensive and time-consuming compared to protein-based analysis.

Although a rapid and cheap technique, ZooMS analysis still typically takes days to conduct and the associated analytical and instrumental costs can escalate for assemblages with hundreds of samples. Analyses of aDNA are more expensive and take much longer for handling and sample preparation, as well as more analytical and instrumental time. As such, it is worthwhile to develop a cheap, minimally-destructive and robust technique, which can screen samples for presence of collagen and/or DNA prior to subsequent analyses. Fourier Transform InfraRed (FTIR) spectroscopy, being a cheap, rapid (analysis completed within minutes) and minimally-destructive analytical technique, is uniquely suitable for such screening.

FTIR spectroscopy is a vibrational spectroscopic technique, which produces the infrared spectrum of a solid, liquid or gas. It is primarily used for identifying the functional groups present in various molecules, with each bond absorbing radiation of a particular frequency/energy (Barbara, 2004). Although FTIR analysis can be carried out solid, liquid, or gaseous samples, most archaeological samples are in solid taste, and FTIR analysis in archaeology have traditionally been carried out by the use of KBr pellets, where the solid samples are ground along with KBr and pressed into a pellet (Lebon et al., 2010; Lee-Thorp and Sponheimer, 2003; Nielsen-Marsh and Hedges, 2000; Trueman et al., 2004; Weiner and Bar-Yosef, 1990; Wright and Schwarcz, 1996). However, Attenuated Total Reflection (ATR) has become increasingly popular as an analytical technique for the analysis of solid and/or liquid samples, owing to its ability to directly analyse minute sample quantities without any sample preparation (Dal Sasso et al., 2016; Hollund et al., 2013; Kontopoulos et al., 2018, 2019; Lebon et al., 2016; Stathopoulou et al., 2008; Thompson et al., 2009). Further, variations in procedures involved in preparation of KBr pellets can influence the FTIR spectrum obtained (Asscher et al., 2011a, 2011b; Surovell and Stiner, 2001), and KBR being hygroscopic, analysis involving KBr pellets can require extensive sample preparation to minimize the influence of moisture in sample measurement.

ATR-FTIR spectroscopy utilises total internal reflection, where a beam of infrared radiation is passed through a crystal present in contact with the sample. The refractive index of the crystal is greater than that of the sample, and the beam is incident, such that it undergoes at least one internal reflection on the crystal-surface interface. This reflection results in an evanescent wave, which penetrates the sample to a small penetration depth (0.5–5 μm) and the resultant evanescent wave is altered in the region of the electromagnetic spectrum where the sample absorbs energy (Mirabella, 1985). The attenuated energy of the evanescent wave affects the infrared beam, which exits the crystal after multiple internal reflections and reaches the detector.

FTIR spectroscopy has been widely used to study archaeological bones, primarily with regard to the various diagenetic alterations resulting in physical, chemical, mechanical, and histological alterations in archaeological bones (Dal Sasso et al., 2016; Lee-Thorp and Sponheimer, 2003; Stathopoulou et al., 2008; Surovell and Stiner, 2001). Such FTIR based indices have been most commonly used to study the changes in bone crystallinity, with the infrared splitting factor (IRSF; also referred to as the Crystallinity Index; $CI = \frac{A_{565}+A_{605}}{A_{595}}$ (Shemesh, 1990; Weiner and Bar-Yosef, 1990; Wright and Schwarcz, 1996); commonly used as a proxy to evaluate the crystal structure of the bone, with a higher value indicating the presence of larger apatite crystals (Shemesh, 1990; Weiner and Bar-Yosef, 1990; Wright and Schwarcz, 1996). The inorganic mineral phase of the bone has been further studied using the C/P ratio of absorbances ($\frac{A_{1415}}{A_{1015}}$, $\frac{\nu_3 CO_3}{\nu_3 PO_4}$; Nielsen-Marsh and Hedges, 2000; Wright and Schwarcz, 1996), which estimates the carbonate content of the bioapatite and can be used to study bone diagenesis and preservation (France et al., 2020; Kontopoulos et al., 2019; Regert et al., 2003; Sponheimer and Lee-Thorp, 1999) and determine the exogenous calcium phosphate incorporated during diagenetic processes (Szostek et al., 2011).

Apart from diagenetic alterations, FTIR spectroscopy has also been widely used to study heat-induced changes in archaeological bones to study heat-induced physico-chemical transformations. Such analysis have focused on the various compositional and structural changes taking place in bones on heating (Munro et al., 2007; Stiner et al., 1995; Thompson et al., 2009), and how the various spectral parameters can be used to differentiate between burned/non-burned bones (Lebon et al., 2008; Mamede et al., 2018; Marques et al., 2018; Shahack-Gross et al., 1997), and the structure of heated/burned bone and the modes of heating involved (Snoeck et al., 2014, 2016).

Apart from the structure of the inorganic phase, FTIR has also been used to study the organic content of the bone, including determining the secondary structure of collagen in archaeological bones (Chadefaux et al., 2009) and estimating the organic content of the bones (Kontopoulos et al., 2020; Lebon et al., 2016; Trueman et al., 2004), with a high correlation observed between the organic/mineral weight and the Am/P ratio of the absorbances ($\frac{Amide\ I}{\nu_3 PO_4}$; Trueman et al., 2004). The Am/P ratio has been previously used as a screening parameter for estimating the insoluble collagen yield prior to paleoproteomic studies (Kontopoulos et al., 2020; Lebon et al., 2016), along with the use of Am/C_1 ($\frac{Amide\ I}{\nu_3 CO_3}$) and Am/$C_2$ ($\frac{Amide\ I}{\nu_2 CO_3}$) peaks, with successful identification of 96–98% of the samples with collagen weight% exceeding 3% and successful elimination of 80–90% of the samples with collagen weight % below 2% (the exact success % depending on the indices used and whether 2% or 3% is used as a collagen weight threshold; (Kontopoulos et al., 2020).

Studies have also looked at how sample preparation, in particular the particle size due to grinding affects the FTIR data, with standard procedures (for e.g. choice of specific bone tissues, grinding procedures, use of grinding curves, filtering particles using molecular size sieves, and baseline correction of the spectra obtained) proposed for improving accuracy, reliability, consistency and replicability of the FTIR data, both in the KBR pellet (Asscher et al., 2011a; Surovell and Stiner, 2001) as well as in the ATR-FTIR modes (Kontopoulos et al., 2018).

FTIR spectroscopy (KBr sample preparation method) has previously been used to study heat-induced changes in the organic and mineral phases of the bone, and it has been suggested that heat-induced

changes in the collagen and mineral phases of the bone can be correlated with the integrity of the DNA, hence leading to a potential screening method in forensics (Fredericks et al., 2012). Recently, the IRSF calculated using ATR-FTIR has been used to screen archaeological bone samples based on aDNA, with the IRSF being able to identify 90–100% of the samples with endogenous content greater than 10%, 80–100% of the samples with DNA content >1% and eliminating 50–70% of the samples with DNA yield <1% (something which can improve to 85% if collagen yield is used as an additional parameter; Kontopoulos et al., 2020).

Apart from FTIR, related spectral techniques like Raman spectroscopy (France et al., 2014; Pestle et al., 2015) and near-infrared spectroscopy (NIR; Sponheimer et al., 2019) have also been used for screening archaeological bones for collagen content. Other methods employed as screening techniques to predict collagen preservation in archaeological bones include percent nitrogen (%N) content and C:N (carbon:nitrogen atomic weight) ratios of bone powder (Brock et al., 2010, 2012; Kim et al., 2011), sulfur speciation mapping (measured using synchrotron-based X-ray fluorescence (XRF) imaging and X-ray absorption spectroscopy (XAS)) (Anné et al., 2019), Ca/F (calcium-to-fluorine ratio; measured using laser-induced breakdown spectroscopy; Rusak et al., 2011), combined X-ray and thermal neutron radiography (Sołtysiak et al., 2018), and micro-computed tomography imaging and porosity measurements (Tripp et al., 2018). However, apart from FTIR, Raman, and NIR measurements, most of the techniques mentioned above are destructive techniques and are not suitable for adaptation to fieldwork. Moreover, the techniques mentioned above mostly focused on screening of bone collagen for isotopic analysis, and as such have solely focused on the insoluble collagen content.

The methods for screening of bones for preservation of aDNA are usually less well-characterized than that for proteins. Aspartic acid racemization was the first approach widely used for screening bones for presence aDNA (Poinar et al., 1996); however, it was later suggested that it was not effective as a screening technique, with Collins et al. (2009) finding no correlation between the D/L values and the success of DNA amplification. Some other screening techniques have also been suggested for ancient DNA, including histology and morphological preservation (Haynes et al., 2002), collagen content (Sosa et al., 2013), crystallinity (Götherström et al., 2002; Sosa et al., 2013), flash pyrolysis GC-MS to identify diketopiperazine-based protein degradation products (Poinar and Stankiewicz, 1999), and the presence of osteocalcin (Smith et al., 2005); however, none of these methods have seen widespread acceptance. Recently, an FTIR-based screening approach has been developed, using thresholds for the IRSF, the C/P ratio, and the collagen wt. %, despite the weak correlation between them and the aDNA yield (Kontopoulos et al., 2020). Out of all the techniques discussed above, only the FTIR-based techniques are suitable to be adapted for fieldwork.

However, despite the advances in using FTIR-based techniques as a screening test for archaeological bones, such studies have mostly focused on the screening of bones for the insoluble collagen content. Contrary to radiocarbon analysis, ZooMS analysis can be performed on the soluble collagen content (and indeed can be argued that it is preferable to perform ZooMS analysis on the soluble fraction, since it enables one to perform further analysis on the insoluble fraction). The application of such FTIR-based screening for the purpose of ZooMS analysis using the soluble collagen is rare, and the few studies undertaken so far shows extremely variable results. Pothier Bouchard and coworkers have used ATR-FTIR spectroscopy to screen bones prior to ZooMS analysis, with different instruments and different ways to estimate CO/P ratios (using peak height and peak areas), but unlike the high success rates for predicting the insoluble collagen content, such analysis have resulted in varying predictive accuracy (Pothier Bouchard et al., 2019). They have suggested that although it is "nearly impossible" to create a universal ATR-FTIR-based screening method for ZooMS with a fixed threshold, an instrument-specific screening method can potentially be developed by calibrating the instrument and combining various methods of calculating the CO/P ratios (Pothier Bouchard et al., 2019). However, further studies involving this approach have suffered from low success rate, with a study involving the Protio-Aurignacian levels from Riparo Bombrini only showing a success rate ~40% when ATR-FTIR was used to screen bones prior to ZooMS analysis (Pothier Bouchard et al., 2020). Previous work has also suggested that in addition to using CO/P values for predicting the presence of soluble collagen in bones, other measurements, such as the position of the Amide I peak, could also prove useful (Pal Chowdhury et al., 2019a,b).

As discussed before, although prior studies have shown that multiple spectral indices can be successfully used for predicting the insoluble collagen content (and the DNA content), such success is not replicated when it comes to screening bones for soluble collagen content prior to ZooMS analysis. In this study, we utilize a decision tree-based machine learning approach to determine whether combining multiple spectral parameters (considering position of certain peaks and ratios between specific peaks simultaneously, as opposed to single Am/P or Am/C ratios) improves the performance ATR-FTIR as a screening test prior to ZooMS collagen fingerprint analysis, without involving extensive sample preparation (e.g. choosing of specific bone tissues, filtering bone powder based on particle size, etc.). To further determine the validity of our approach, we also investigated whether ATR-FTIR, combined with a decision tree-based machine learning approach can be utilized as a screening test for aDNA extracted from bones based on spectral parameters without undertaking extensive spectral data manipulation.

2. Materials and methods

The archaeological bones used in this study included marine and terrestrial mammalian bones, obtained from a number of different sites around the world, ranging from Upper Palaeolithic to the modern period. We chose sites which differed in location, chronology, taxonomic, and preservational context to ensure any screening method thus developed was applicable for a wide range of samples belonging to different chronological periods and different depositional environments.

Primarily, three different archaeological assemblages were included in this study. Firstly, terrestrial mammalian bone fragments (n = 187) were obtained from recent excavations (2011–16) at Grotte Mandrin, a Middle and Upper Palaeolithic rock shelter in the Auvergne-Rhône-Alpes region of modern France (Slimak, 2008). Multiple stratigraphic layers (layers A-I) have been excavated, with a rich and diverse archaeological record, including faunal and macrofaunal remains (including hominin remains), lithics, and other evidence of extensive human occupation (Higham et al., 2014; Romandini et al., 2014; Slimak et al., 2017). The site is generally well-preserved, with geoarchaeological analyses revealing layers A-D to be in "good" and layers E-H (the bone fragments for the present study were from Layer E) to be in "excellent" preservation condition (Higham et al., 2014; Romandini et al., 2014). Secondly, we included previously published data of 452 bone fragments from Proto-Aurignacian levels A1 and A2 at Riparo Bombrini (Balzi Rossi; Pothier Bouchard et al., 2020), a well-dated and well-documented Middle-Upper Palaeolithic rock shelter located on the Ligurian coast (Italy) immediately east of the border with France (Formicola, 1989; Riel-Salvatore et al., 2013; Higham et al., 2014; Benazzi et al., 2015; Riel-Salvatore and Negrino, 2018a, 2018b; Holt et al., 2019). The Proto-Aurignacian levels spanning 42ky-36 ky cal BP have revealed dense occupations of the site as shown by high concentrations of lithic and faunal remains and the presence of overlaying *cuvette*-type hearths (Holt et al., 2019; Riel-Salvatore and Negrino, 2018b). Riparo Bombrini is also one of the rare sites to have yielded diagnostic *Homo sapiens* remains in secure Proto-Aurignacian context (Formicola, 1989; Benazzi et al., 2015). However, the

analysis of faunal remains from the site is extremely challenging, because of the high degree of bone fragmentation (mostly dry fractures) as well as the variable nature of collagen preservation (Pothier Bouchard et al, 2019, 2020).

Lastly, to both extend the taxonomic range of FTIR-based screening prior to ZooMS and to consider its utility to screen for ancient DNA (aDNA), we analysed a younger set of skeletal remains collected primarily from six multi-period archaeological sites across Orkney and Shetland (henceforth referred to as the North Atlantic dataset). These samples were dominated by cetacean bones, and represent approximately 25% of the cetacean samples collected by a broader study focused on analysis of marine mammal use within pre-modern North Atlantic history (Szabo, unpublished data). Most samples come from six sites dating from middle to late Iron Age (although some of the samples were undated) through to the Norse period and excavated between the 1930s and 2018. Several samples were also taken from 12 early modern and modern whaling stations or stranding sites across the North Atlantic. Bones from two Orkney sites, the Iron Age ritual site of Mine Howe, Tankerness, Orkney (Card et al., 2005; Card and Downes, 2003) and from the multi-phase Iron Age broch and roundhouse at The Cairns, Windwick Bay (Carruthers, 2019) were found across multiple contexts within which organic materials were well-preserved, indicating good preservational condition. In contrast, the samples from Jarlshof, Shetland (Hamilton, 1956) and Gurness, Orkney (Hedges, 1987), were excavated in the early twentieth century, when minimal attention was given to recording the preservation or analysis of cetacean bones. Across these sites some marine mammal bone has been analysed morphologically, but cetacean bone has remained largely unexamined by either element or species, owing to its highly worked and fragmentary nature. Species identification of cetaceans found on archaeological sites is a prerequisite to consideration of economic or cultural value of these animals, thereby making biomolecular analysis a critical exercise for post-excavation analysis.

3. Experimental details

3.1. Sampling strategy

For FTIR and ZooMS analysis of Set II, III and IV approximately 30–50 mg of bone powder were either drilled using dentist's ProTaper tools or and removed from each specimen or ground in a pestle and mortar and stored at room temperature. The bones were nor subject to any detailed pretreatment, with only any externally adhering soil and surface debris being removed. For *Set*I (and IA), a cordless electric drill was used to collect the bone powder, and no drill rate was determined. For the DNA analysis, approximately 300–500 mg of bone shavings were collected from specimens as per Mcleod et al. (2008) and stored at −20 °C until subsequent analysis. The results from ATR-FTIR, ZooMS and DNA analyses were integrated and analysed using machine learning to develop models to use FTIR as a predictive tool for ZooMS and aDNA analysis, with the results of the screening being verified against whether the samples furnished collagen in ZooMS analysis or aDNA as applicable.

3.2. FTIR

Approximately 2–5 mg of bone powder was removed from each specimen for ATR-FTIR analysis. A PerkinElmer Spotlight 400 FTIR Imaging System and Universal Spectrometer, with the spectral range set between 650 and 3500 cm^{-1}, was used to analyse 98 North Atlantic cetacean samples (*Set*I) and the 187 terrestrial mammalian bone fragments from Grotte Mandrin (Set II); 16 scans were performed for every sample and a background measurement was carried out before every sample measurement. FTIR spectra of the 187 Grotte Mandrin bones were also collected using a Bruker Opus Spectrometer with an ATR platinum Diamond 1 Refl #CFA4832D accessory (Set III; 36 scans, transmittance mode, 400-4000 cm^{-1}) and used for model building to determine whether a universal ATR-FTIR-based screening method for the presence of collagen can be developed irrespective of the instrument involved. Prior published ATR-FTIR data from 451 bone fragments from Riparo Bombrini were also used to further cross-validate our model-building approach (Set IV; Pothier Bouchard et al., 2019, 2020). The samples from Riparo Bombrini were analysed using a portable Agilent 4500a FTIR instrument, equipped with a single-bounce diamond ATR and internal battery (64 scans, absorbance mode, full range 4000–650 cm^{-1}). For investigating whether ATR-FTIR can be used to screen for the presence of DNA, a subset of the cetacean bone fragments (n = 87) were considered for model building and validation purposes (Set IA).

3.3. ZooMS collagen fingerprinting

Collagen from the bones was extracted and analysed based on the method developed by Buckley and colleagues (Buckley et al., 2009; van der Sluis et al., 2014). Briefly, the bone powder (30–50 mg) was demineralised using 0.6 M HCl for 18 h at 4 °C, and the supernatant liquid was collected and ultrafiltered for 15 min at 12400 RPM. The retentate was further ultrafiltered into 500 μl of 50 mM ammonium bicarbonate (ABC) twice, redissolved in 100 μl of ABC, and digested using 0.4 μg of trypsin for 18 h. The resultant peptides were diluted using 0.1% trifluoroacetic acid (TFA) (1:20 v/v) and spotted for MALDI analysis on a ground-steel target plate along with an equal volume of α-cyano-4-hydroxycinnamic acid (10 mg/ml in 50% acetonitrile (ACN) as matrix. The samples were analysed using a Bruker Autoflex TOF/TOF spectrometer, accumulating 1000 scans per sample and maintaining the laser power at 45%.

3.4. Ancient DNA analysis

All aDNA handling protocols and DNA extraction methodology followed protocols previously outlined in Rastogi et al. (2004) and Mcleod et al. (2008). Presence of analysable DNA was confirmed through the successful amplification and sequencing of three fragments of the mitochondrial DNA (mtDNA) of varying lengths (~186–445 basepairs (bp)). The three fragments were: 1) a ~445 basepair (bp) fragment of the cytochrome *b* gene (using primers CBCet4F (5′ ACA TGG ACT TCA ACC ATG AC 3′) and CBCet5R (5′ CTC AGA ATG ATA TTT GTC CTC AGG 3′)); 2) a ~345 bp fragment of the control region (using primers T-Pro and Primer-2); and 3) a ~186 bp fragment of the cytochrome *b* gene (using primers CBCet4F and CBCet1R (5′ GTA TTG CTA GAA ATA GGC C 3′)). For all mtDNA PCR amplifications we used a 15 μl reaction volume containing 2 μl DNA extract (of unknown DNA concentration): 1x PCR buffer (Promega), 0.2 Mm each dNTP (Invitrogen), 0.3 μg/μl UltraPureTM BSA (Invitrogen), 1.5 mM MgCl, 0.3 μM each primer, and 0.1U/μl Taq (Promega). PCR cycling conditions consisted of an initial 5-min denaturation step at 94 °C; 50 cycles of 94 °C for 30 s, 50 °C for 1 min, and 72 °C for 1 min; and a final extension step at 60 °C for 45 min. All PCR product was evaluated for quantity and quality using agarose electrophoresis, then prepared for sequencing, cycle sequenced, and size separated and visualised on an ABI 3500xl Genetic Analyzer (Applied Biosystems) after McLeod et al. (2014). All samples were sequenced in both directions (e.g., with both primers of the primer pair used for amplification). Sequences were then examined visually using 4 Peaks v1.8 (Nucleobytes.com), and edited and aligned in MEGA7 v7.0.26 (Kumar et al. 2016). Each sequence was then confirmed as cetacean in origin through BLAST (www.ncbi.nlm.nih.gov/blast/; Johnson et al., 2008), with identification confirmed only if criteria of 100% query coverage and 95% max identity were confirmed. Species identity was also confirmed through phylogenetic analysis as

part of a larger research project. However, for the purposes of this study successful DNA amplification and confirmation of DNA product as cetacean was logged as 'Pass/Fail' data.

4. Data analysis and modelling

4.1. ZooMS data

The MALDI spectral files were converted to. mzxml files using Bruker CompassXport utility and analysed using mMass 5.5.0 (Niedermeyer and Strohalm, 2012). The baseline was corrected using a baseline correction value of 15, and automatic peak picking was carried out with a signal-to-noise ratio of 3 and picking height of 75. The spectra which furnished the mammalian biomarker peak at *m/z* 1105 (and the corresponding deamidated peak at *m/z* 1106) and one of the collagen species-specific biomarkers 'B' or 'C' were considered to have yielded collagen (Pal Chowdhury et al., 2019a,b; for naming of peptides see Buckley et al., 2009).

4.2. ATR-FTIR spectral data

The FTIR spectral data were analysed using ACD Spectrus software. After applying ATR correction and baseline subtraction, the peaks were identified using auto peak picking with wavenumber in the x-axis and absorbance in the y-axis. The peak heights were used to determine absorbances corresponding to the following peaks: Amide I of collagen (-C═O stretching, 1590-1710 cm^{-1}; Lebon et al., 2016); phosphate (-P═O antisymmetric stretching (ν_3 PO_4), ~1015 cm^{-1} (Stutman et al., 1965; Trueman et al., 2004);) and carbonate (-C═O antisymmetric stretching (ν_3 CO_3), ~1415 cm^{-1}; Wright and Schwarcz, 1996). The absorbances due to the various peaks were used to calculate the following four quantities:

1. Amide-I-to-carbonate ratio ($\frac{Amide\ I}{\nu_3 CO_3}$; (Trueman et al., 2004)Kontopoulos et al., 2020)
2. Amide-I-to-phosphate ratio ($\frac{Amide\ I}{\nu_3 PO_4}$; (Trueman et al., 2004))
3. Organic-to-inorganic ratio (also referred to as the Amide-I-to-inorganic ratio, $\frac{Amide\ I}{\nu_3 PO_4 + \nu_3 CO_3}$)
4. Carbonate-to-phosphate ratio ($\frac{\nu_3 CO_3}{\nu_3 PO_4}$; (Wright and Schwarcz, 1996)).

Along with the four ratios mentioned above, the positions and intensities of the Amide 1, carbonate and phosphate peaks were used as parameters to predict for presence of collagen and DNA using decision tree-based learning methods. All decision tree-based prediction models were coded using Python and visualised using Dataiku Data Science Studio (https://www.dataiku.com/product/). Scatter plots and boxplots, where applicable, were created using R in the RStudio development environment.

4.3. Decision tree-based models for use of ATR-FTIR As A screening technique

A decision tree is a decision support system, which takes a flow-chart-like form, with each internal node representing a point where an attribute or a property is checked (a test), and the branches from a node indicating the results of that test based on which of the samples are further divided into groups (further nodes; see Fig. 1; Breiman et al., 1984; Morgan and Sonquist, 1963). For our models we used ensemble learning, where multiple shallow decision trees (each having a limited number of nodes) were created and combined using the soft-voting approach (for an overview of ensemble learning, see Dietterich, 2002). Random Forest was the ensemble learning technique used in this model, where multiple decision trees are created and combined by using a subset of parameters and bagging of the available data (explained later) at any given time (Breiman, 2001; Ho, 1995).

The working of the individual tree represented in Fig. 1 is explained as follows:

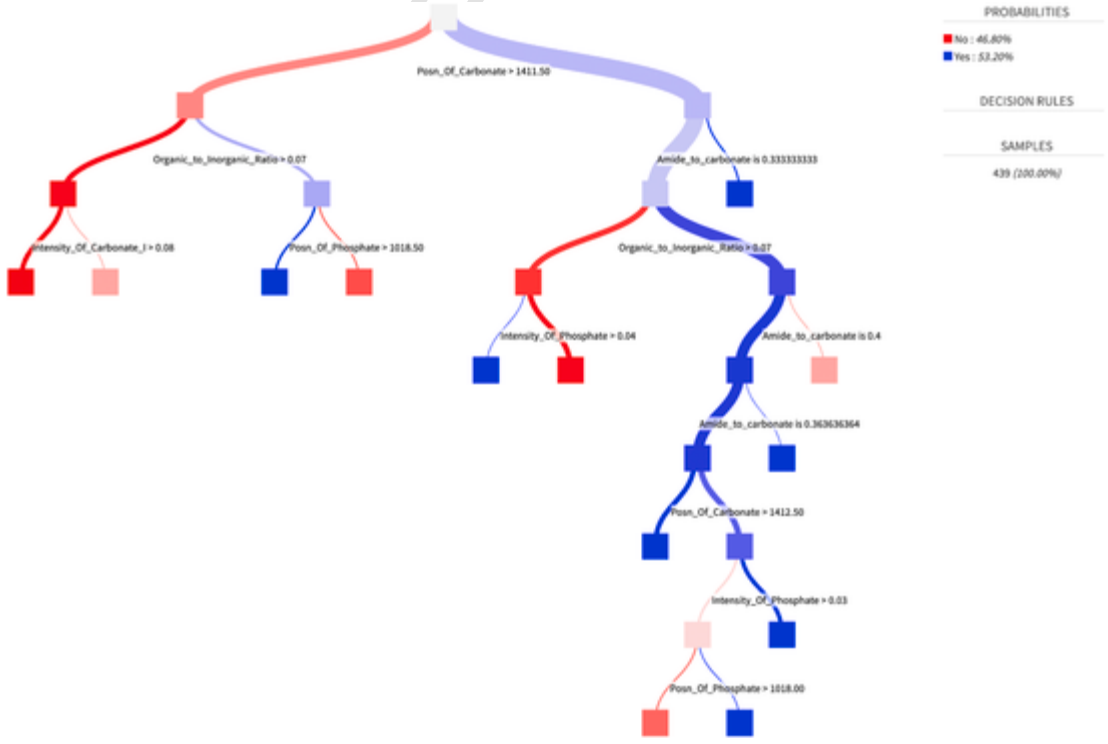

Fig. 1. A singled out decision tree out of the ensemble created in one of the models (model A) for using ATR-FTIR as a screening prior to ZooMS analysis. Each model has multiple such decision trees, differing slightly.

Initially, the position of carbonate is used as a decision-making parameter, with a value greater than 1411.50 indicating presence of collagen. If the value of this parameter is less than 1411.50, it is tentatively classified as not yielding collagen, with organic-to-inorganic ratio used as the subsequent parameter in that case. An organic-to-inorganic ratio greater than 0.07 indicates a possibility of collagen, with this being followed by the position of phosphate as the next parameter, where a value greater than 1018.50 indicates the presence of collagen. The rest of the decision tree can be read and interpreted in a similar way, with the intensity of carbonate being used as the next parameter for the samples with organic-to-inorganic ratio less than 0.07. Similarly, the samples with position of carbonate greater than 1411.50 have amide-to-carbonate being used as the next parameter, and so on. Throughout the tree, the blue and red nodes/branches represent a yes/no response respectively, with the shading indicating the qualitative degree of confidence in the classification.

However, it is to be noted that this is an isolated example of a single tree which is a part of the ensemble which makes up a model (model A in this example), and many such trees collectively formed the final iteration of our models. The number of trees in the model is a hyperparameter usually denoted by N, the value of which is obtained by tuning the hyperparameters iteratively (100 and 150 for this work depending on the model). Further, due to the randomisation of the parameters (explained below) each decision tree is slightly different. As such, the individual values/parameters mentioned in the trees are of little physical significance, and by themselves cannot be used to generate cut-off values or thresholds for predicting the presence or absence of collagen.

The decision trees created in this study were all shallow trees (e.g., Fig. 1), making them 'weak learners'. However, since multiple such trees converged to a single decision (without individual trees having all the essential nodes, which represent tests with the parameters involved in the decision-making process), it proved the robustness of the model (Breiman, 2001). This approach also reduced the risk of overfitting, which is a possibility associated with the use of deep trees. Bootstrapping and random selection of features were utilized to ensure the process of generating decision tree parameters is randomised. Using bootstrapping, the datasets were initially sampled using the 'random with replacement' approach, which ensured that not every tree sees all of the dataset. Of the parameters being used, some were randomly removed at various nodes, ensuring the tree is optimised for a random set of parameters, and not merely the best-case scenario (Breiman, 1996, 2001). The resultant decision from each tree was based on a probability figure, and multiple such trees were combined to create a model (Breiman, 2001).

For combining the multiple trees created, two distinct approaches can be used:

1. Hard Voting - In this approach the resultant probability figure from each tree is considered, a threshold applied, and all probabilities above that pre-determined threshold are assigned to a category. The resulting final classification from each tree is recorded, and a simple frequency count is used to combine the results of various trees and arrive at a decision based on simple majority voting (Delgado and Ishii, 1999). However, this approach results in loss of probabilistic information corresponding to the individual trees.
2. Soft Voting - In soft voting the resultant probability figures from multiple decision trees are averaged and the threshold is applied to the averaged probability. The final classification is based on the averaged probability (Wang et al., 2013).

In this work we combined the trees based on the soft-voting approach.

Once a model is created, its performance can be measured based on the following indicators (Kent et al., 1955).

1. Accuracy (*acc.*), which is the fraction of accurately predicted occurrences among all the data, $acc = \frac{True\ Positive+True\ Negative}{True\ Positive+True\ Negative+False\ Positive+False\ Negative}$
2. Precision (p), which is the fraction of actual occurrences among all the predicted occurrences, expressed as $p = \frac{True\ Positive}{True\ Positive+False\ Positive}$
3. Recall (r), which is the fraction of occurrences that were accurately predicted by the model, expressed as $r = \frac{True\ Positive}{True\ Positive+Flase\ Negative}$
4. F1 score, which is the harmonic mean of the precision and recall values, expressed as $F1 = \frac{2pr}{p+r}$ (Chinchor, 1992)

For any model dealing with imbalanced data, where one of either the positive or the negative significantly outnumbers the other, precision and recall are considered better metrics for evaluating the model performance as compared to accuracy. Further, use of F1 value instead of accuracy also ensures that the false positives and false negatives affect the success of the model (they are ignored when only accuracy is considered). In this work we consider F1 score, the harmonic mean of precision and recall values as the primary parameter for evaluating the success of the models (see Chinchor, 1992).

5. Results

Previous attempts at using ATR-FTIR as a screening test prior to ZooMS analysis of archaeological bones focused on Amide-I-to–phosphate ratio as the primary predictive parameter under consideration (Pal Chowdhury et al., 2019a,b; Pothier Bouchard et al., 2019, 2020), along with potential use of the position of the Amide I peak (Pal Chowdhury et al., 2019a,b). For comparison to this previous work, here we also present boxplots for all datasets involved in this study computed by grouping the calculated Amide-I-to-phosphate ratios based on whether the bones yielded collagen or not in order to determine if that ratio can be used to develop a universal predictive cut-off, irrespective of sites or instruments involved (Fig. 2). Scatter plots were also plotted for this data, with the position of the Amide I peak on the x axis and the Amide-I-to-phosphate ratio on the y axis to determine whether there is any relationship between the position of the Amide I peak and the possibility of the bones yielding collagen (Fig. 3).

As evident from the boxplots, the use of Amide-I-to-phosphate ratio as the sole parameter makes it extremely challenging to develop a precise universal screening approach. Different sites and instruments lead to different cut-off ratios, and there was considerable overlap of the Amide-I-to-phosphate values between the samples which yielded collagen and the samples that did not. This overlap was particularly prominent in dataset IV (the assemblage from Riparo Bombrini), which reduced the possibility of any meaningful screening based on this ratio alone.

The scatter plots presented in Fig. 3 furthermore showed that the position of the Amide I peak was unlikely to be a predictor for the presence of collagen in archaeological bones. Although in one of the assemblages (dataset IV), the Amide I peak for the samples which did not yield collagen was concentrated on the lower end of the wavenumber range (1600-1630 cm^{-1}), this trend was not reproduced in the other assemblages. To better use ATR-FTIR spectra as a screening test for proteins prior to ZooMS analysis, we used the eight previously mentioned parameters to create models using a random forest-based machine learning approach.

Initially, three models were created, described as follows:

Model A: The IR data from *Set*I and II were combined into one unified dataset, and the resultant dataset was randomly split into training and test sets in a 4:1 ratio.

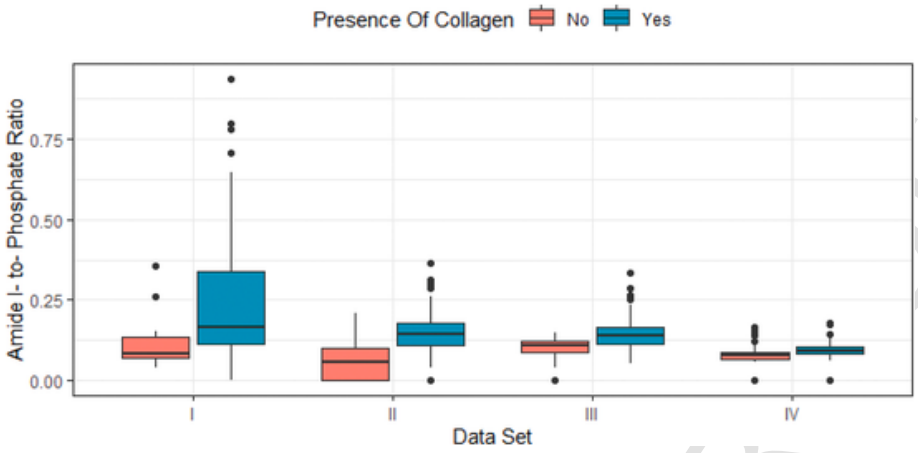

Fig. 2. Box plots showing the Amide I-to-phosphate ratios for the various datasets analysed in this study. Two data points (14.4 and 1.48) from *Set*I were removed while plotting box plots to ensure the plots remained to scale.

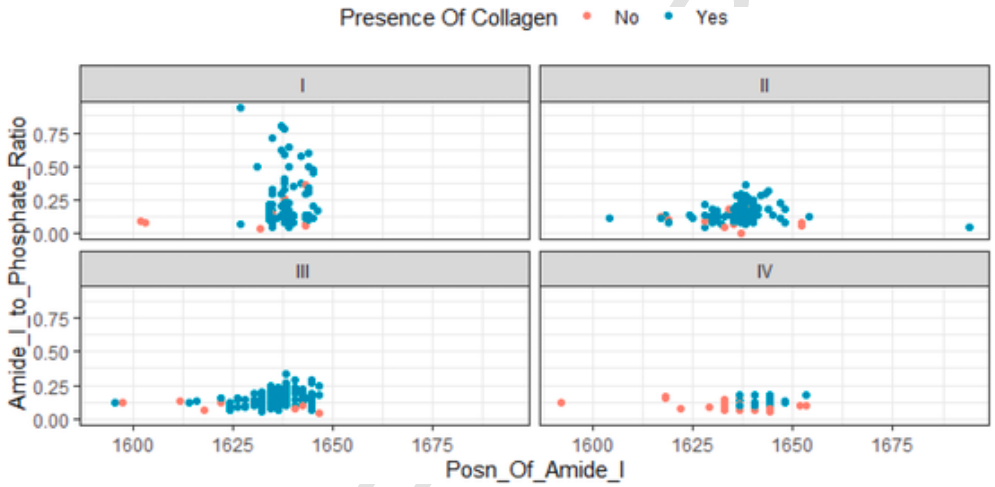

Fig. 3. Scatter plots of the Amide I-to-phosphate ratios against the position of the Amide I peaks for the various datasets analysed in this study.

Model B: Trained on the IR data of *Set*I and tested on the IR data of Set II.

Model C: Trained on the IR data of Set II and tested on the IR data of *Set*I.

Once the models were developed, IR data corresponding to Set III were used to calculate the F1, *p* and *r* scores to compare the models for their predictive ability (Table 1).

The results outlined in Table 1 showed that the decision tree-based approach is potentially useful in applying ATR-FTIR as a screening technique, independent of the spectrometer used. When only the well-preserved bones are used as training and test sets, the F1 scores of the various models are in the range of 90–96%, indicating a robust method with high levels of accuracy, precision and recall. However, all the bones in Sets I, II, and II were from sites with good preservational conditions, evident from the geoarchaeological investigations and preservation of organic remains in Mandrin and the preservation of DNA and organic remains in most of the North Atlantic sample sites. To further determine whether this method can be extended to multiple sites in different preservational conditions, we used IR and MALDI spectra of bone fragments from Riparo Bombrini (Set IV), a site with very poor preservation (as opposed to the Mandrin and North Atlantic bones) to cross-validate this approach. Further, the Set IV data were also recorded with a portable instrument instead of a table-top one (as in Sets I, II, and III) thus having the added advantage of extending the applicability of the method to portable instruments used in fields. Along with the sampling and measurement protocol, the energy source, detector type, and the spectral resolution will affect the spectral data (Soriano-Disla et al., 2017), possibly leading to differences between portable and table-top instruments.

Despite previous successes for well-preserved sites, analysis of poorly preserved bones from Riparo Bombrini showed extremely poor results for the use of ATR-FTIR as a screening technique, with F1 scores ranging from 42.42% to 63.00% depending on the model used (Table 1). We postulated this drop in accuracy was due to difference in the nature of the training data (which was from samples with excellent preservation) and the testing data (from samples with poor preservation). To test this, three further models were built:

Model D: Trained on the Riparo Bombrini (Set IV) dataset and tested on *Set*I and II combined.

Model E: The Riparo Bombrini dataset (Set IV) was randomly split into training and test sets in a 4:1 ratio.

Model F: The Riparo Bombrini, North Atlantic, and the Grotte Mandrin dataset (sets I, II, and IV) were combined into one unified dataset, and the resultant dataset was randomly split into training and test sets in a 4:1 ratio.

Model D, which had a large difference in the preservational quality of the training and test data, gave an F1 score of 52.80%, whereas Model E, where both the training and test datasets had similar preservational quality, gave an F1 score of 89.86% (Table 2). This suggested the similarity (or difference) in the nature of the training and the test

Table 1
The various assemblages of archaeological bones analysed in this study. For collagen, success and failure refers to whether soluble collagen was successfully obtained from the sample and identified using MALDI. For DNA, success and failure represents whether DNA was successfully extracted from the sample and confirmed as cetacean in origin.

Molecule Analysed	Assemblage	ATR-FTIR Spectrometer	N	Successes	Failures
Collagen	North Atlantic Cetaceans	Perkin Elmer Spotlight 400 FTIR Imaging System (*Set*I)	98	87	11
	Grotte Mandrin	Perkin Elmer Spotlight 400 FTIR Imaging System (Set II) Bruker Opus Spectrometer with an ATR platinum Diamond 1 Refl #CFA4832D (Set III)	187	164	23
	Riparo Bombrini	Agilent 4500a potable FTIR (Set IV))	451	185	266
DNA	North Atlantic Cetaceans	Perkin Elmer Spotlight 400 FTIR Imaging System (Set IA)	87	49	38

data plays an important role in determining the success of the model. However, it is to be noted that all decision tree-based methods resulted in a slight improvement in screening of the bones from Riparo Bombrini sites compared to manual use of the Amide-I-to-phosphate ratio, which gave a ~41% predictive success (Pothier Bouchard et al., 2020) (see Table 3).

To make our model universally applicable, we further combined the available data from all study sites (sets I, II and IV; set III was excluded so as not to include the same samples twice) and split the combined dataset in a 4:1 ratio, using the larger subset as training and the smaller subset as test data (Model F). This substantially improved the model, with *p*, *r*, and F1 scores of 83.70%, 87.50%, and 85.70% respectively. We credit this improvement to the similarity in the training and test data, prerequisite for successful machine learning models.

To determine whether FTIR spectroscopy can be used as a screening test prior to DNA analysis, a model was created using the IR data from Set IA (a subset of North Atlantic samples, n = 87) by randomly splitting the data into training and test sets (4:1 ratio). The parameters used were the same as those used for collagen screening, but with the additional presence/absence of collagen (based on the ZooMS results; see section 4.1 for the criteria) as a new parameter. The *p*, *r* and F1 values obtained from this model were respectively 72.73%, 100.00%, and 84.21%, indicating that this approach can be used as an effective screening technique for DNA (Table 4).

6. Discussion

Our results show that random forest-based machine learning approaches can be an effective for ATR-FTIR-based screening of archaeological bones prior to ZooMS and/or aDNA analysis by combining multiple IR spectral parameters. Previous investigations for use of ATR-FTIR as a screening test focused on the Amide-I-to-phosphate ratio as the sole screening parameter. However, for our machine learning-based models the most important variable in predicting the presence of collagen differed from model to model. Although Amide-I-to-phosphate ratio (along with organic-to-inorganic ratio) was among the top three most important variables in a majority of the models, we also noticed significant contributions from the Amide-I-to-carbonate ratio and carbonate-to-phosphate ratios, along with other parameters (Figs. 4 and 5; Supplementary Figures S1-4).

In the variable dependency charts a variable with a higher value contributes towards making a larger part of the decision. As mentioned previously, each model involves the generation of N number of uncorrelated decision trees and a final decision is made based on the 'soft majority' vote. This allows the models to better generalise the decision-making process, but makes them sensitive to the parameters and configurations involved in the training, which lead to possible changes in the respective importance of the variables.

The variable dependency charts also show that in some charts some variables appear multiple times with different values (e.g., Figs. 4 and 5 & Supplementary Figures S1-S4). A variable, which appears only once in the dependency chart, indicates that the variable contributes to the decision, but for multiple trees multiple values of the variable are used in the decision-making process. On the contrary, a variable, for which differing values appear on the chart, indicates that those specific values have been used by a majority of the trees in the decision-making process. It is also to be noted that the individual values mentioned in the variable dependency charts are of little physical importance due to the randomisation of parameters described previously.

7. Conclusions and future work

Our models presented here conclusively improve on the accuracy of usage of FTIR as a prior screening technique for ZooMS by applying decision tree-based methods. We also show that this approach potentially allows for a universal screening system, applicable across multiple sites and largely independent of the spectrometers used. The method also does not require extensive sample selection and preparation steps, allowing for quick screening on field involving portable spectrometers. The predictive power of such approaches is greatly dependent on the preservational quality of the sites and we suggest two possible approaches taking this into account:

Data from well-preserved and poorly-preserved sites can be treated separately, with different modelling systems used for each (Model A for well-preserved sites and Model E for poorly-preserved sites). This approach provides the highest accuracy (F1 scores from 89.8% to 94%).

Table 2
The various indicators used in determining the predictive capacity of the models A, B, and C.

Model	Test Set (%)				Set III (%)				Set IV (%)			
	acc.	p	R	F1	acc.	p	r	F1	acc.	p	R	F1
A	92.98	92.73	100.00	96.23	90.42	90.32	100.00	94.91	54.99	47.50	93.50	63.00
B	92.48	95.74	95.81	95.73	86.17	90.34	94.64	92.44	70.28	66.00	56.75	61.00
C	83.38	93.61	87.38	90.35	83.51	91.51	89.88	90.06	66.29	70.88	30.00	42.42

Table 3
The various indicators involved in determining the predictive capacity of the models D, E and F.

	acc. (%)	*P (%)*	*R (%)*	F1 (%)
Model D	42.16	93.39%	36.75%	52.80%
Model E	92.22	88.57%	91.18%	89.86%
Model F	82.31	83.70%	87.50%	85.70%

Table 4
The various indicators involved in determining the predictive capacity of the models D, E and F.

acc. (%)	*P (%)*	*R (%)*	F1 (%)
84.21	72.73	100.00	84.21

The IR data of bone fragments, irrespective of their preservational state, can also be analysed by our combined Model F. This approach simplifies the screening by using a single model but provides for a slightly reduced success rate (F1 = 85.70% for our test data).

We also show that a similar tree-based approach is potentially applicable for the screening of DNA, but a larger dataset needs to be analysed before specific conclusions can be drawn and effective models built for screening to give the highest success rates.

Uncited reference

Wadsworth et al., 2017.

Declaration of competing interest

None.

Acknowledgements

The authors thank the Royal Society for support and funding a research fellowship to M.B (UF120473), the Natural Environment Research Council for funding of the PerkinElmer FTIR (grant number NE/J023426/1) and the University of Manchester, Faculty of Science and Engineering for a President's Doctoral Scholarship to M.P.C. The authors also thank the "Soprintendenza Archeologia, Belle Arti e Paesaggio" and the "Polo Museale della Liguria" for facilitating and supporting fieldwork in Liguria. J.R. and F.N. acknowledges the Université de Montréal, the University of Genoa, the Fonds Québécois pour la Recherche – Société et Culture (grant 2016-NP-193048) and the Social Sciences and Humanities Research Council of Canada (Insight Grant 435-2017-1520) for funding recent excavations at Riparo Bombrini. S.B. acknowledges the European Research Council (ERC) for funding excavations at Riparo Bombrini under the European Union's Horizon 2020 research and innovation programme (grant agreement No 724046). V.S. and B. F. also thank Nick Card, Ingrid Mainland and Martin Carruthers of the University of the Highlands and Islands for assistance with the North Atlantic specimens included in this manuscript, as

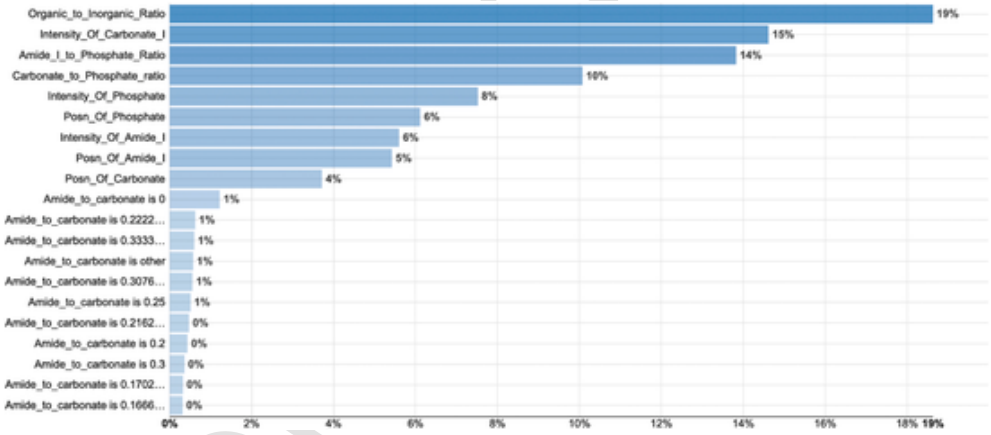

Fig. 4. Variable dependency chart for Model F (for Models A-E see Supplementary Figures S1-4).

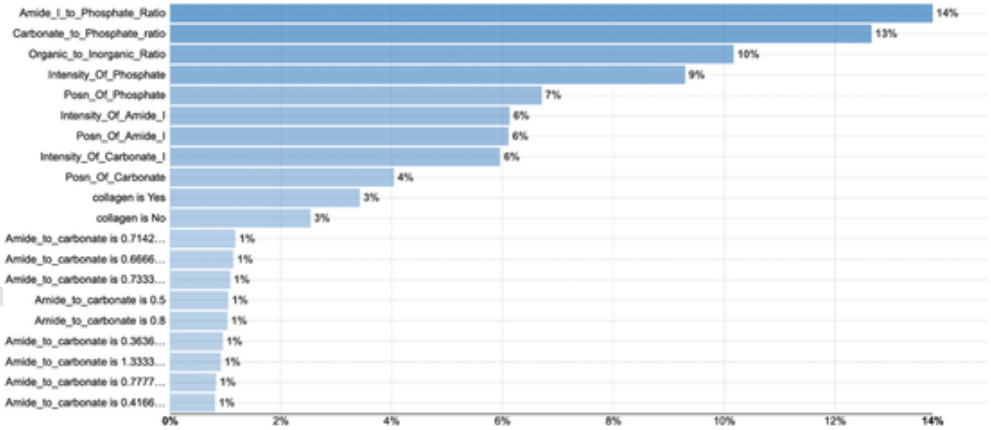

Fig. 5. Variable dependency chart for the decision tree-based model created to screen for presence of aDNA. Note the multiple Amide-I-to-carbonate values (0.7142, 0.6666, and so on), indicating that those specific values have been used by a majority of the trees in the decision-making process.

well as the National Science Foundation for funding (Arctic Social Science program; grant award #1503714).

Appendix A. Supplementary data

Supplementary data to this article can be found online at https://doi.org/10.1016/j.jas.2020.105311.

References

Anné, J., Edwards, N.P., Brigidi, F., Gueriau, P., Harvey, V.L., Geraki, K., Slimak, L., Buckley, M., Wogelius, R.A., 2019. Advances in bone preservation: identifying possible collagen preservation using sulfur speciation mapping. Palaeogeogr. Palaeoclimatol. Palaeoecol. 520, 181–187.

Asscher, Y., Regev, L., Weiner, S., Boaretto, E., 2011a. Atomic disorder in Fossil TooThand bone mineral: an FTIR study using the grinding curve method. ArchéoSciences 35, 135–141. doi:10.4000/archeosciences.3062.

Asscher, Y., Weiner, S., Boaretto, E., 2011b. Variations in atomic disorder in biogenic carbonate hydroxyapatite using the infrared spectrum grinding curve method. Adv. Funct. Mater. 21, 3308–3313. doi:10.1002/adfm.201100266.

Barbara, S., 2004. Infrared Spectroscopy: Fundamentals and Applications. John Wiley & Sons., Chichester, West sussex.

Benazzi, S., Slon, V., Talamo, S., Negrino, F., Peresani, M., Bailey, S.E., Sawyer, S., Panetta, D., Vicino, G., Starnini, E., Mannino, M.A., Salvadori, P.A., Meyer, M., Pääbo, S., Hublin, J.J., 2015. The makers of the Protoaurignacian and implications for Neandertal extinction. Science 348, 793–796. doi:10.1126/science.aaa2773.

Bläuer, A., Kantanen, J., 2013. Transition from hunting to animal husbandry in Southern, Western and Eastern Finland: new dated osteological evidence. J. Archaeol. Sci. 40, 1646–1666. doi:10.1016/j.jas.2012.10.033.

Bocherens, H., Tresset, A., Wiedemann, F., Giligny, F., Lafage, F., Lanchol, m Y., Mariotti, A., 1997. Diagenetic evolution of mammal bones in two French Neolithic sites. Bull. la Société Géologique Fr. 168, 555–564.

Bocherens, H., Mashkour, M., Billiou, D., Pellé, E., Mariotti, A., 2001. A new approach for studying prehistoric herd management in arid areas: intra-tooth isotopic analyses of archaeological caprine from Iran. Comptes Rendus l'Académie des Sci. - Ser. IIA - Earth Planet. Sci. 332, 67–74.

Boskey, A.L., 2007. Mineralization of bones and teeth. Elements 3, 385–391.

Boskey, A.L., 2013. Bone composition: relationship to bone fragility and antiosteoporotic drug effects. BoneKEy Rep. 2. doi:10.1038/bonekey.2013.181.

Breiman, L., 1996. Bagging predictors. Mach. Learn. 24, 123–140.

Breiman, L., 2001. Random forests. Mach. Learn. 45, 5–32.

Breiman, L., Friedman, J.H., Olshen, R.A., Stone, C.J., 1984. Classification and Regression Trees. Chapman and Hall/CRC.

Brock, F., Higham, T., Ramsey, C.B., 2010. Pre-screening techniques for identification of samples suitable for radiocarbon dating of poorly preserved bones. J. Archaeol. Sci. 37, 855–865.

Brock, F., Wood, R., Higham, T.F.G., Ditchfield, P., Bayliss, A., Ramsey, C.B., 2012. Reliability of nitrogen content (%N) and carbon:nitrogen atomic ratios (C:N) as indicators of collagen preservation suitable for radiocarbon dating. Radiocarbon 53, 879–886.

Buckley, M., 2018. Zooarchaeology by mass spectrometry (ZooMS) collagen fingerprinting for the species identification of archaeological bone fragments. In: Zooarchaeology in Practice. Springer, Cham, pp. 227–247.

Buckley, M., Collins, M., Thomas-Oaies, J., Wilson, J.C., 2009. Species identification by analysis of bone collagen using matrix-assisted laser desorption/ionisation time-of-flight mass spectrometry. Rapid Commun. Mass Spectrom. 23, 3843–3854. doi:10.1002/rcm.4316.

Buckley, M., Whitcher Kansa, S., Howard, S., Campbell, S., Thomas-Oates, J., Collins, M., 2010. Distinguishing between archaeological sheep and goat bones using a single collagen peptide. J. Archaeol. Sci. 37, 13–20. doi:10.1016/j.jas.2009.08.020.

Campos, P.F., Craig, O.E., Turner-Walker, G., Peacock, E., Willerslev, E., Gilbert, M.T.P., 2012. DNA in ancient bone - where is it located and how should we extract it? Ann. Anat. 194, 7–16.

Card, N., Downes, J., 2003. Mine Howe- the significance of space and place in the Iron Age. In: Downs, J., Ritchie, A. (Eds.), Sea Change, Orkney and Northern Europe in the Later Iron Age AD 300-800. Pinkfoot Press, pp. 11–19.

Card, N., Downes, J., Gibson, J., Sharman, P., 2005. The mine Howe environs project. Curr. Archaeol. 199, 322–327.

Carruthers, M., 2019. The Cairns dig diary 2019. Univ. Highl. Islands Archaeol. Inst. [WWW Document] https://archaeologyorkney.com/category/the-cairns-dig-diary-2019/ (accessed 6.11.20).

Chadefaux, C., Hô, A. Le, Bellot-gurlet, L., Ina, R., 2009. Curve-Fitting micro-atr-ftir studies of the amide I and Ii bands of type I collagen in archaeological bone materials. e-Preservation Sci. 6, 129–137.

Chinchor, N., 1992. MUC-4 evaluation metrics. In: Proceedings of the Fourth Message Understanding Conference. p. 22. doi:10.3115/1072064.1072067.

Clutton-Brock, J., 1979. The mammalian remains from the Jericho Tell. Proc. Prehist. Soc. 45, 135–157. doi:10.1017/S0079497X00009713.

Collins, M.J., Riley, M.S., Child, A.M., Turner-Walker, G., 1995. A basic mathematical simulation of the chemical degradation of ancient collagen. J. Archaeol. Sci. 22, 175–183.

Collins, M.J., Nielsen-Marsh, C.M., Hiller, J., Smith, C.I., Roberts, J.P., Prigodich, R.V., Wess, T.J., Csapò, J., Millard, A.R., Turner-Walker, G., 2002. The survival of organic matter in bone: a review. Archaeometry 44, 383–394.

Collins, M.J., Penkman, K.E.H., Rohland, N., Shapiro, B., Dobberstein, R.C., Ritz-Timme, S., Hofreiter, M., 2009. Is amino acid racemization a useful tool for screening for ancient DNA in bone? Proc. R. Soc. B Biol. Sci. 276, 2971–2977.

Crabtree, P.J., 1990. Zooarchaeology and complex societies: some uses of faunal analysis for the study of trade, social status. Archaeol. Method Theor. 2, 155–205.

Dal Sasso, G., Lebon, M., Angelini, I., Maritan, L., Usai, D., Artioli, G., 2016. Bone diagenesis variability among multiple burial phases at Al Khiday (Sudan) investigated by ATR-FTIR spectroscopy. Palaeogeogr. Palaeoclimatol. Palaeoecol. 463, 168–179. doi:10.1016/j.palaeo.2016.10.005.

de Jong, W.F., 1926. La Substance Minérale Dans les Os. 45, 445–448.

Delgado, J., Ishii, N., 1999. Memory-based weighted-majority prediction for recommender systems. In: Proceedings of ACM SIGIR '99 Workshop Recommender Systems: Algorithms and Evaluation.

Dietterich, T.G., 2002. Ensemble learning. In: Arbib, M.A. (Ed.), The Handbook of Brain Theory and Neural Networks. MIT Press, Cambridge, Masachusetts.

Domínguez-Rodrigo, M., Bunn, H.T., Mabulla, A.Z.P., Baquedano, E., Uribelarrea, D., Pérez-González, A., Gidna, A., Yravedra, J., Diez-Martin, F., Egeland, C.P., Barba, R., Arriaza, M.C., Organista, E., Ansón, M., 2014. On meat eating and human evolution: a taphonomic analysis of BK4b (Upper Bed II, Olduvai Gorge, Tanzania), and its bearing on hominin megafaunal consumption. Quat. Int. 322, 129–152. doi:10.1016/j.quaint.2013.08.015.

Eglinton, G.E., Logan, G.A., 1991. Molecular preservation. Philos. Trans. R. Soc. B Biol. Sci. 333, 315–328.

France, C.A.M., Thomas, D.B., Doney, C.R., Madden, O., 2014. FT-Raman spectroscopy as a method for screening collagen diagenesis in bone. J. Archaeol. Sci. 42, 346–355.

France, C.A.M., Sugiyama, N., Aguayo, E., 2020. Establishing a preservation index for bone, dentin, and enamel bioapatite mineral using ATR-FTIR. J. Archaeol. Sci. Rep. 33, 102551. doi:10.1016/j.jasrep.2020.102551.

Fredericks, J.D., Bennett, P., Williams, A., Rogers, K.D., 2012. FTIR spectroscopy: a new diagnostic tool to aid DNA analysis from heated bone. Forensic Sci. Int. Genet. 6, 375–380. doi:10.1016/j.fsigen.2011.07.014.

Gordon, C.C., Buikstra, J.E., 1981. Soil pH, bone preservation, and sampling bias at Mortuary sites. Am. Antiq. 46, 566–571.

Götherström, A., Collins, M.J., Angerbjörn, A., Lidén, K., 2002. Bone preservation and DNA amplification. Archaeometry 44, 395–404.

Gruss, L.T., Schmitt, D., 2015. The evolution of the human pelvis: changing adaptations to bipedalism, obstetrics and thermoregulation. Philos. Trans. R. Soc. B Biol. Sci.. doi:10.1098/rstb.2014.0063.

Halstead, P., Isaakidou, V., 2017. Calf mortality and milking: was Tony Legge right after all? In: Rowley-conwy, P., Serjeantson, D., Halstead, P. (Eds.), Economic Zooarchaeology: Studies in Hunting, Herding and Early Agriculture. Oxbow Books.

Hamilton, J.R.C., 1956. Excavations at Jarlshof. Shetland, Edinburgh.

Harvey, V.L., Egerton, V.M., Chamberlain, A.T., Manning, P.L., Buckley, M., 2016. Collagen fingerprinting: a new screening technique for radiocarbon dating ancient bone. PloS One 11 (3), e0150650.

Haynes, S., Searle, J.B., Bretman, A., Dobney, K.M., 2002. Bone preservation and ancient DNA: the application of screening methods for predicting DNA survival. J. Archaeol. Sci. 29, 585–592.

Hedges, J.W., 1987. Bu, Gurness and the brochs of Orkney: part 2 [monograph]. Br. Archaeol. Rep. 164.

Hedges, R.E.M., Millard, A.R., Pike, A.W.G., 1995. Measurements and relationships of diagenetic alteration of bone from three archaeological sites. J. Archaeol. Sci. 22, 201–209.

Herries, A.I.R., Martin, J.M., Leece, A.B., Adams, J.W., Boschian, G., Joannes-Boyau, R., Edwards, T.R., Mallett, T., Massey, J., Murszewski, A., Neubauer, S., Pickering, R., Strait, D.S., Armstrong, B.J., Baker, S., Caruana, M.V., Denham, T., Hellstrom, J., Moggi-Cecchi, J., Mokobane, S., Penzo-Kajewski, P., Rovinsky, D.S., Schwartz, G.T., Stammers, R.C., Wilson, C., Woodhead, J., Menter, C., 2020. Contemporaneity of australopithecus, paranthropus, and early homo erectus in South Africa. Science 80, 368. doi:10.1126/science.aaw7293.

Higham, T., Douka, K., Wood, R., Ramsey, C.B., Brock, F., Basell, L., Camps, M., Arrizabalaga, A., Baena, J., Barroso-Ruíz, C., Bergman, C., Boitard, C., Boscato, P., Caparrós, M., Conard, N.J., Draily, C., Froment, A., Galván, B., Gambassini, P., Garcia-Moreno, A., Grimaldi, S., Haesaerts, P., Holt, B., Iriarte-Chiapusso, M.J., Jelinek, A., Jordá Pardo, J.F., Maíllo-Fernández, J.M., Marom, A., Maroto, J., Menéndez, M., Metz, L., Morin, E., Moroni, A., Negrino, F., Panagopoulou, E., Peresani, M., Pirson, S., De La Rasilla, M., Riel-Salvatore, J., Ronchitelli, A., Santamaria, D., Semal, P., Slimak, L., Soler, J., Soler, N., Villaluenga, A., Pinhasi, R., Jacobi, R., 2014. The timing and spatiotemporal patterning of Neanderthal disappearance. Nature 512, 306–309. doi:10.1038/nature13621.

Ho, T.K., 1995. Random decision forests. In: Proceedings of the International Conference on Document Analysis and Recognition. Institute of Electrical and Electronic Engineers, Montreal, pp. 278–282.

Hollund, H.I., Ariese, F., Fernandes, R., Jans, M.M.E., Kars, H., 2013. Testing an alternative high-throughput tool for investigating bone diagenesis: ftir in attenuated total reflection (atr) mode. Archaeometry. doi:10.1111/j.1475-4754.2012.00695.x.

Holt, B., Negrino, F., Riel-Salvatore, J., Formicola, V., Arellano, A., Arobba, D., Boschian, G., Churchill, S.E., Cristiani, E., Di Canzio, E., Vicino, G., 2019. The middle-upper Paleolithic transition in Northwest Italy: new evidence from Riparo Bombrini (Balzi Rossi, Liguria, Italy). Quat. Int. 508, 142–152. doi:10.1016/j.quaint.2018.11.032.

Johnson, M., Zaretskaya, I., Raytselis, Y., Merezhuk, Y., McGinnis, S., Madden, T.L., 2008. NCBI blast: a better web interface. Nucleic Acids Res. 36.

Kent, A., Berry, M.M., Luehrs, F.U., Perry, J.W., 1955. Machine literature searching VIII. Operational criteria for designing information retrieval ssytems. J. Assoc. Inf. Sci. Technol. 6, 93–101.

Kim, K.J., Wong, W., Park, J.H., Woo, H.J., Hodgins, G., Jull, A.J.T., Lee, Y.J., Kim, J.Y., 2011. Development of radiocarbon dating method for degraded bone samples from Korean archaeological sites. Radiocarbon 53, 129–135.

Kitamura, H., Iwamoto, C., Sakairi, N., Tokura, S., Nishi, N., 1997. Marked effect of DNA on collagen fibrillogenesis in vitro. Int. J. Biol. Macromol. 20, 241–244. doi:10.1016/S0141-8130(97)00021-4.

Kontopoulos, I., Presslee, S., Penkman, K., Collins, M.J., 2018. Preparation of bone powder for FTIR-ATR analysis: the particle size effect. Vib. Spectrosc. 99, 167–177. doi:10.1016/j.vibspec.2018.09.004.

Kontopoulos, I., Penkman, K., Liritzis, I., Collins, M.J., 2019. Bone diagenesis in a Mycenaean secondary burial (Kastrouli, Greece). Archaeol. Anthropol. Sci. 11, 5213–5230. doi:10.1007/s12520-019-00853-0.

Kontopoulos, I., Penkman, K., Mullin, V.E., Winkelbach, L., Unterländer, M., Scheu, A., Kreutzer, S., Hansen, H.B., Margaryan, A., Teasdale, M.D., Gehlen, B., Street, M., Lynnerup, N., Liritzis, I., Sampson, A., Papageorgopoulou, C., Allentoft, M.E., Burger, J., Bradley, D.G., Collins, M.J., 2020. Screening archaeological bone for palaeogenetic and palaeoproteomic studies. PloS One 15, e0235146. doi:10.1371/journal.pone.0235146.

Kusaka, S., 2019. Stable isotope analysis of human bone hydroxyapatite and collagen for the reconstruction of dietary patterns of hunter-gatherers from Jomon populations. Int. J. Osteoarchaeol. 29, 36–47.

Lebon, M., Reiche, I., Fröhlich, F., Bahain, J.J., Falguères, C., 2008. Characterization of archaeological burnt bones: contribution of a new analytical protocol based on derivative FTIR spectroscopy and curve fitting of the ν 1 ν 3 PO4 domain. Anal. Bioanal. Chem. 392, 1479–1488. doi:10.1007/s00216-008-2469-y.

Lebon, M., Reiche, I., Bahain, J.J., Chadefaux, C., Moigne, A.M., Fröhlich, F., Sémah, F., Schwarcz, H.P., Falguères, C., 2010. New parameters for the characterization of diagenetic alterations and heat-induced changes of fossil bone mineral using Fourier transform infrared spectrometry. J. Archaeol. Sci. 37, 2265–2276. doi:10.1016/j.jas.2010.03.024.

Lebon, M., Reiche, I., Gallet, X., Bellot-Gurlet, L., Zazzo, A., 2016. Rapid quantification of bone collagen content by ATR-FTIR spectroscopy. Radiocarbon 58, 131–145. doi:10.1017/RDC.2015.11.

Lee-Thorp, J., Sponheimer, M., 2003. Three case studies used to reassess the reliability of fossil bone and enamel isotope signals for paleodietary studies. J. Anthropol. Archaeol. 22, 208–216. doi:10.1016/S0278-4165(03)00035-7.

Lee-Thorp, J.A., Sealy, J.C., van der Merwe, N.J., 1989. Stable carbon isotope ratio differences between bone collagen and bone apatite, and their relationship to diet. J. Archaeol. Sci. 16, 585–599.

LeGeros, R.Z., 1981. Apatites in biological systems. Prog. Cryst. Growth Char. 4, 1–45.

Lewis, M.C., Sealy, J.C., 2018. Coastal complexity: ancient human diets inferred from Bayesian stable isotope mixing models and a primate analogue. PloS One 13, e02094111. doi:10.1371/journal.pone.0209411.

Lindahl, T., 1993. Instability and decay of the primary structure of DNA. Nature 362, 709–715.

Mamede, A.P., Vassalo, A.R., Piga, G., Cunha, E., Parker, S.F., Marques, M.P.M., Batista De Carvalho, L.A.E., Gonçalves, D., 2018. Potential of bioapatite hydroxyls for research on archeological burned bone. Anal. Chem. 90, 11556–11563. doi:10.1021/acs.analchem.8b02868.

Marín, J., Saladié, P., Rodríguez-Hidalgo, A., Carbonell, E., 2017. Neanderthal hunting strategies inferred from mortality profiles within the Abric Romaní sequence. PloS One. doi:10.1371/journal.pone.0186970.

Marques, M.P.M., Mamede, A.P., Vassalo, A.R., Makhoul, C., Cunha, E., Gonçalves, D., Parker, S.F., Batista de Carvalho, L.A.E., 2018. Heat-induced bone diagenesis probed by vibrational spectroscopy. Sci. Rep. 8, 1–13. doi:10.1038/s41598-018-34376-w.

Mcleod, B.A., Brown, M.W., Moore, M.J., Stevens, W., Barkham, S.H., Barkham, M., White, B.N., 2008. Bowhead whales, and not right whales, were the primary target of 16th- to 17th-century Basque whalers in the western North Atlantic. Arctic 61, 61–75.

McLeod, B.A., Frasier, T.R., Lucas, Z., 2014. Assessment of the extirpated Maritimes walrus using morphological and ancient DNA analysis. PloS One 9, e99569. doi:10.1371/journal.pone.0099569.

Mirabella, F.M., 1985. Internal reflection spectroscopy. Appl. Spectrosc. Rev. 21, 45–178.

Morgan, J.N., Sonquist, J.A., 1963. Problems in the analysis of survey data, and A proposal. J. Am. Stat. Assoc. 58, 415–434.

Munro, L.E., Longstaffe, F.J., White, C.D., 2007. Burning and boiling of modern deer bone: effects on crystallinity and oxygen isotope composition of bioapatite phosphate. Palaeogeogr. Palaeoclimatol. Palaeoecol. 249, 90–102. doi:10.1016/j.palaeo.2007.01.011.

Munson, P.J., 2000. Age-correlated differential destruction of bones and its effect on Archaeological mortality profiles of domestic sheep and goats. J. Archaeol. Sci. 27, 391–407. doi:10.1006/jasc.1999.0463.

Napierala, H., Uerpmann, H.P., 2012. A "new" palaeolithic dog from central Europe. Int. J. Osteoarchaeol. 22, 127–137. doi:10.1002/oa.1182.

Newesely, H., 1989. Fossil bone apatite. Appl. Geochem. 4, 233–245.

Niedermeyer, T.H.J., Strohalm, M., 2012. mMass as a software tool for the annotation of cyclic peptide tandem mass spectra. PloS One 7. doi:10.1371/journal.pone.0044913.

Nielsen-Marsh, C.M., Hedges, R.E.M., 1999. Bone porosity and the use of mercury intrusion porosimetry in bone diagenesis studies. Archaeometry 41, 165–174.

Nielsen-Marsh, C.M., Hedges, R.E.M., 2000. Patterns of diagenesis in bone I: the effects of site environments. J. Archaeol. Sci. 27, 1139–1150. doi:10.1006/jasc.1999.0537.

Nielsen-Marsh, C., Gernaey, A., Turner-Walker, G., Hedges, R., Pike, A.W.G., Collins, M., 2000. The chemical degradation of bone. In: Cox, M., Mays, S. (Eds.), Human Osteology: in Archaeology and Forensic Science. Cambridge University Press, Cambridge, GB, pp. 439–454.

Nielsen-Marsh, C.M., Smith, C.I., Jans, M.M.E., Nord, A., Kars, H., Collins, M.J., 2007. Bone diagenesis in the European Holocene II: taphonomic and environmental considerations. J. Archaeol. Sci. 34, 1523–1531.

Okazaki, M., Yoshida, Y., Yamaguchi, S., Kaneno, M., Elliott, J.C., 2001. Affinity binding phenomena of DNA onto apatite crystals. Biomaterials 22, 2459–2464.

Pal Chowdhury, M., Wogelius, R., Manning, P.L., Metz, L., Slimak, L., Buckley, M., 2019a. Collagen deamidation in archaeological bone as an assessment for relative decay rates. Archaeometry arcm 12492. doi:10.1111/arcm.12492.

Pal Chowdhury, Manasij, Wogelius, R., Manning, P., Metz, L., Slimak, L., Buckley, M., 2019b. Collagen deamidation in archaeological bones as an assessment for relative decay rates. Archaeometry 61, 1382–1398.

Payne, S., 1985. Morphological distinctions between the mandibular teeth of young sheep, Ovis, and goats, Capra. J. Archaeol. Sci. 12, 139–147. doi:10.1016/0305-4403(85)90058-5.

Perkins, D., 1973. The beginnings of animal domestication in the near east. Am. J. Archaeol. 77, 279–282.

Pestle, W.J., Brennan, V., Sierra, R.L., Smith, E.K., Vesper, B.J., Cordell, G.A., Colvard, M.D., 2015. Hand-held Raman spectroscopy as a pre-screening tool for archaeological bone. J. Archaeol. Sci. 58, 113–120.

Poinar, H.N., Stankiewicz, B.A., 1999. Protein preservation and DNA retrieval from ancient tissues. Proc. Natl. Acad. Sci. U.S.A. 96, 8426–8431.

Poinar, H.N., Höss, M., Bada, J.L., Pääbo, S., 1996. Amino acid racemization and the preservation of ancient DNA. Science (80-.) 272, 864–866.

Pothier Bouchard, G., Mentzer, S.M., Riel-Salvatore, J., Hodgkins, J., Miller, C.E., Negrino, F., Wogelius, R., Buckley, M., 2019. Portable FTIR for on-site screening of archaeological bone intended for ZooMS collagen fingerprint analysis. J. Archaeol. Sci. Rep. 26, 101862. doi:10.1016/J.JASREP.2019.05.027.

Pothier Bouchard, G., Riel-Salvatore, J., Negrino, F., Buckley, M., 2020. Archaeozoological, taphonomic and ZooMS insights into the Protoaurignacian faunal record from Riparo Bombrini. Quat. Int. 1. doi:10.1016/j.quaint.2020.01.007.

Rastogi, T., Brown, M.W., McLeod, B.A., Frasier, T.R., Grenier, R., Cumbaa, S.L., Nadarajah, J., White, B.N., 2004. Genetic analysis of 16th-century whale bones prompts a revision of the impact of Basque whaling on right and bowhead whales in the western North Atlantic. Can. J. Zool. 82, 1647–1654.

Regert, M., Vacher, S., Moulherat, C., Decavallas, O., 2003. Adhesive production and pottery function during the Iron Age at the site of grand aunay (Sarthe, France). Archaeometry 45, 101–120. doi:10.1111/1475-4754.00098.

Reitz, E.J., 1987. Vertebrate fauna and socioeconomic status. In: Spencer-Wood, S.M. (Ed.), Consumer Choice in Historical Archaeology. Springer Science + Business Media, New York, pp. 101–120. doi:10.1007/978-1-4757-9817-3.

Riel-Salvatore, J., Negrino, F., 2018a. Human adaptations to climatic change in Liguria across the middle–upper Paleolithic transition. J. Quat. Sci. 33, 313–322.

Riel-Salvatore, J., Negrino, F., 2018b. Proto-aurignacian lithic technology, mobility, and human Niche construction: a case study from Riparo Bombrini, Italy. In: Robinson, E., Sellet, F. (Eds.), Lithic Technological Organization and Paleoenvironmental Change Global and Diachronic Perspectives. Springer Nature, pp. 163–188.

Riel-Salvatore, J., Ludeke, I.C., Negrino, F., Holt, B.M., 2013. A spatial analysis of the late mousterian levels of Riparo Bombini (Balzi Rossi, Italy). Can. J. Archaeol. 37, 70–92.

Rofes, J., Garcia-Ibaibarriaga, N., Aguirre, M., Martínez-García, B., Ortega, L., Zuluaga, M.C., Bailon, S., Alonso-Olazabal, A., Castaños, J., Murelaga, X., 2015. Combining small-vertebrate, marine and stable-isotope data to reconstruct past environments. Sci. Rep. 5, 14219. doi:10.1038/srep14219.

Romandini, M., Peresani, M., Laroulandie, V., Metz, L., Pastoors, A., Vaquero, M., Slimak, L., 2014. Convergent evidence of eagle talons used by late Neanderthals in Europe: a further assessment on symbolism. PloS One 9. doi:10.1371/journal.pone.0101278.

Rusak, D.A., Marsico, R.M., Taroli, B.L., 2011. Using laser-induced breakdown spectroscopy to assess preservation quality of archaeological bones by measurement of calcium-to-fluorine ratios. Appl. Spectrosc. 65, 1193–1196.

Samei, S., Alizadeh, K., Munro, N.D., 2019. Animal husbandry and food provisioning at the Kura-Araxes settlement of Köhne Shahar in Northwestern Iran. J. Anthropol. Archaeol. 55, 101065. doi:10.1016/j.jaa.2019.05.001.

Schoeninger, M.J., 2014. Stable isotope analyses and the evolution of human diets. Annu. Rev. Anthropol. 43, 413–430.

Shahack-Gross, R., Bar-Yosef, O., Weiner, S., 1997. Black-coloured bones in Hayonim Cave, Israel: differentiating between burning and oxide staining. J. Archaeol. Sci. 24, 439–446. doi:10.1006/jasc.1996.0128.

Shemesh, A., 1990. Crystalinity and diagenesis of sedimentary apatites. Geochim. Cosmochim. Acta 2433–2438.

Slimak, L., 2008. The Neronian and the historical structure of cultural shifts from middle to upper palaeolithic in Mediterranean France. J. Archaeol. Sci. 35, 2204–2214. doi:10.1016/J.JAS.2008.02.005.

Slimak, L., Belkacem, D., Belles, F., Bonneau, A., Brochier, J.É., Brugal, J.-P., Buckley, M., Camus, H., Coqueugniot, H., Condemi, S., Crégut-Bonnoure, E., De Beaulieu, J.-L., Desmars, A., Djamali, M., Dutour, O., Frouin, M., Giraud, Y., Grenet, M., Higham, T., Lacrampe-Cuyaubère, F., Longet, B., Pal Chowdhury, M., Wogelius, R., Mercier, N., Metz, L., Muth, X., Seguin-Orlando, A., Orlando, L., Rabanit, M., Roussel, A., Schwenninger, J.-L., Sikora, M., Vandevelde, S., Willerslev, E., Yvorra, P., 2017. Installations de la fin du Paléolithique moyen de la Grotte Mandrin, Malataverne, (Drôme). Fouille programmée triennale 2015-2017. Rapport de synthèse.

Smith, C.I., Craig, O.E., Prigodich, R.V., Nielsen-Marsh, C.M., Jans, M.M.E., Vermeer, C., Collins, M.J., 2005. Diagenesis and survival of osteocalcin in archaeological bone. J. Archaeol. Sci. 32, 105–113.

Snoeck, C., Lee-Thorp, J.A., Schulting, R.J., 2014. From bone to ash: compositional and structural changes in burned modern and archaeological bone. Palaeogeogr. Palaeoclimatol. Palaeoecol. 416, 55–68. doi:10.1016/j.palaeo.2014.08.002.

Snoeck, C., Schulting, R.J., Lee-Thorp, J.A., Lebon, M., Zazzo, A., 2016. Impact of heating conditions on the carbon and oxygen isotope composition of calcined bone. J. Archaeol. Sci. 65, 32–43. doi:10.1016/j.jas.2015.10.013.

Somerville, A.D., Nelson, B.A., Knudson, K.J., 2010. Isotopic investigation of pre-Hispanic macaw breeding in Northwest Mexico. J. Anthropol. Archaeol. 29, 125–135. doi:10.1016/j.jaa.2009.09.003.

Soriano-Disla, J.M., Janik, L.J., Allen, D.J., McLaughlin, M.J., 2017. Evaluation of the performance of portable visible-infrared instruments for the prediction of soil properties _ Elsevier Enhanced Reader. Biosyst. Eng. 161, 24–36.

Sosa, C., Vispe, E., Núñez, C., Baeta, M., Casalod, Y., Bolea, M., Hedges, R.E.M., Martinez-Jarreta, B., 2013. Association between ancient bone preservation and DNA yield: a multidisciplinary approach. Am. J. Phys. Anthropol. 151, 102–109.

Sołtysiak, A., Mińta-Jakubowska, E.A., Dorosz, M., Kosiński, T., Fijał-Kirejczyk, I., 2018. Estimation of collagen presence in dry bone using combined X-ray and neutron radiography. Appl. Radiat. Isot. 139, 141–145.

Sponheimer, M., Lee-Thorp, J.A., 1999. Alteration of enamel carbonate environments during fossilization. J. Archaeol. Sci. 26, 143–150. doi:10.1006/jasc.1998.0293.

Sponheimer, M., Ryder, C.M., Fewlass, H., Smith, E.K., Pestle, W.J., Talamo, S., 2019. Saving Old Bones: a non-destructive method for bone collagen prescreening. Sci. Rep. 9, 13928. doi:10.1038/s41598-019-50443-2.

Stathopoulou, E.T., Psycharis, V., Chryssikos, G.D., Gionis, V., Theodorou, G., 2008. Bone diagenesis: new data from infrared spectroscopy and X-ray diffraction. Palaeogeogr. Palaeoclimatol. Palaeoecol. 266, 168–174. doi:10.1016/j.palaeo.2008.03.022.

Stephan, E., 2000. Oxygen isotope analysis of animal bone phosphate: method refinement, influence of consolidants, and reconstruction of palaeotemperatures for Holocene sites. J. Archaeol. Sci. 27, 523–535. doi:10.1006/jasc.1999.0480.

Stiner, M.C., Kuhn, S.L., Weiner, S., Bar-Yosef, O., 1995. Differential burning, recrystallization, and fragmentation of archaeological bone. J. Archaeol. Sci. 22, 223–237. doi:10.1006/jasc.1995.0024.

Stiner, M.C., Buitenhuis, H., Duru, G., Kuhn, S.L., Mentzer, S.M., Munro, N.D., Pöllath, N., Quade, J., Tsartsidou, G., Özbaşaran, M., 2014. A forager-herder trade-off, from broad-spectrum hunting to sheep management at Aşikli Höyük, Turkey. Proc. Natl. Acad. Sci. U.S.A. 111, 8404–8409. doi:10.1073/pnas.1322723111.

Stutman, J.M., Termine, J.D., Posner, A.S., 1965. Vibrational spectra and structure of the phosphate ion in some calcium phosphates. Trans. N. Y. Acad. Sci. 27, 669–675. doi:10.1111/j.2164-0947.1965.tb02224.x.

Surovell, T.A., Stiner, M.C., 2001. Standardizing infra-red measures of bone mineral crystallinity: an experimental approach. J. Archaeol. Sci. 28, 633–642. doi:10.1006/jasc.2000.0633.

Szostek, K., Stepańczak, B., Szczepanek, A., Kpa, M., Głąb, H., Jarosz, P., Włodarczak, P., Tunia, K., Pawlyta, J., Paluszkiewicz, C., Tylko, G., 2011. Diagenetic signals from ancient human remains-bioarchaeological applications. Mineralogia 42, 93–112. doi:10.2478/v10002-011-0009-4.

Thompson, T.J.U., Gauthier, M., Islam, M., 2009. The application of a new method of Fourier Transform Infrared Spectroscopy to the analysis of burned bone. J. Archaeol. Sci. 36, 910–914. doi:10.1016/j.jas.2008.11.013.

Tornero, C., Balasse, M., Ughetto-Monfrin, J., Molist, M., Saña, M., 2017. Evaluating seasonality of birth in gazelles in the Middle Euphrates Valley: confirming ethological assumptions in the Abu Hureyra model. In: Rowley-conwy, P., Serjeantson, D., Halstead, P. (Eds.), Economic Zooarchaeology: Studies in Hunting, Herding and Early Agriculture. Oxbow Books.

Tripp, J.A., Squire, M.E., Hedges, R.E.M., Stevens, R.E., 2018. Use of micro-computed tomography imaging and porosity measurements as indicators of collagen preservation in archaeological bone. Palaeogeogr. Palaeoclimatol. Palaeoecol. 511, 462–471.

Trueman, C.N.G., Behrensmeyer, A.K., Tuross, N., Weiner, S., 2004. Mineralogical and compositional changes in bones exposed on soil surfaces in Amboseli National Park, Kenya: diagenetic mechanisms and the role of sediment pore fluids. J. Archaeol. Sci. 31, 721–739. doi:10.1016/j.jas.2003.11.003.

Turner-Walker, G., Parry, T.V., 1995. The tensile strength of archaeological bone. J. Archaeol. Sci. 22, 185–191. doi:10.1006/jasc.1995.0020.

Ungar, P., 2004. Dental topography and diets of Australopithecus afarensis and early Homo. J. Hum. Evol. 46, 605–622. doi:10.1016/j.jhevol.2004.03.004.

van der Merwe, N.J., Vogel, J.C., 1978. 13C Content of human collagen as a measure of prehistoric diet in woodland North America. Nature 276, 815–816.

van der Sluis, L.G., Hollund, H.I., Buckley, M., De Louw, P.G.B., Rijsdijk, K.F., Kars, H., 2014. Combining histology, stable isotope analysis and ZooMS collagen fingerprinting to investigate the taphonomic history and dietary behaviour of extinct giant tortoises from the Mare aux Songes deposit on Mauritius. Palaeogeogr. Palaeoclimatol. Palaeoecol. 416, 80–91. doi:10.1016/j.palaeo.2014.06.003.

Wadsworth, C., Procopio, N., Anderung, C., Carretero, J.M., Iriarte, E., Valdiosera, C., Elburg, R., Penkman, K., Buckley, M., 2017. Comparing ancient DNA survival and proteome content in 69 archaeological cattle tooth and bone samples from multiple European sites. J. Protozool. 158, 1–8.

Wadsworth, C., Buckley, M., 2018. Characterization of proteomes extracted through collagen-based stable isotope and radiocarbon dating methods. J. Proteom. Res. 17, 429–439.

Wang, Haishen, Yang, Y., Wang, Hongjun, Chen, D., 2013. Soft-voting clustering ensemble. In: Zhou, Z.-H., Roli, F., Kittler, J. (Eds.), Multiple Classifier Systems. 11th International Workshop, MCS 2013. Springer, pp. 307–318. doi:10.1109/9780470544600.ch16.

Ward, S., Hill, A., 1987. Pliocene hominid partial mandible from tabarin, Baringo, Kenya. Am. J. Phys. Anthropol. 72, 21–37.

Weiner, S., Bar-Yosef, O., 1990. States of preservation of bones from prehistoric sites in the Near East: a survey. J. Archaeol. Sci. 17, 187–196. doi:10.1016/0305-4403(90)90058-D.

Wright, L.E., Schwarcz, H.P., 1996. Infrared and isotopic evidence for diagenesis of bone apatite at Dos Pilas, Guatemala: Palaeodietary implications. J. Archaeol. Sci. 23, 933–944. doi:10.1006/jasc.1996.0087.

Yeomans, L., Martin, L., Richter, T., 2019. Close companions: early evidence for dogs in northeast Jordan and the potential impact of new hunting methods. J. Anthropol. Archaeol. 53, 161–173. doi:10.1016/j.jaa.2018.12.005.

Zeder, M.A., 1991. Feeding Cities: Specialized Animal Economy in the Ancient Near East. Smithsonian Institution Press, Washington, D.C.

Zeder, M.A., Hesse, B., 2000. The initial domestication of goats (Capra hircus) in the Zagros mountains 10,000 years ago. Science 287, 2254–2257. doi:10.1126/science.287.5461.2254.

Zeder, M.A., Bradley, D.G., Emshwiller, E., Smith, B.D. (Eds.), 2006. Archaeological documentation of animal domestication. In: Documenting Domestication: New Genetic and Archaeological Paradigms. University of California Press, pp. 171–272. doi:10.1663/0013-0001(2006)60[398a:ddngaa]2.0.co;2.